




Relaxation dynamics of Fe₅₅Cr₁₀Mo₁₄C₁₅B₆ metallic glass explored by mechanical spectroscopy and calorimetry measurements

Chaoren Liu¹  · Milad Madinehei¹ · Eloi Pineda²  · Daniel Crespo¹ 

Received: 15 September 2015 / Accepted: 25 February 2016 / Published online: 17 March 2016
© Akadémiai Kiadó, Budapest, Hungary 2016

Abstract In this work, the mechanical relaxation dynamics of Fe₅₅Cr₁₀Mo₁₄C₁₅B₆ metallic glass is explored by mechanical spectroscopy. The temperature-dependent loss modulus $E''(T)$ shows the features of β relaxation well below glass transition temperature T_g . This β relaxation can be well described in the framework of anelastic theory by a thermal activated process with activation energy of 165 kJ mol^{-1} . Structural relaxation, also known as physical aging, has a large effect on the glass properties. The activation energy spectrum of structural relaxation is characterized by differential scanning calorimetry measuring the heat flow difference between as-quenched and relaxed states. The obtained energy spectrum is well described by a lognormal distribution with maximum probability activation energy of 176 kJ mol^{-1} . The obtained activation energy of structural relaxation is similar to that of β relaxation observed from mechanical spectroscopy. Both values are also close to the Johari–Goldstein β relaxation estimated by the empirical rule $E_\beta = 26RT_g$.

Keywords Metallic glass · Viscosity · Mechanical relaxation · Anelastic · Physical aging · Structural relaxation

Introduction

Fe-based metallic glasses (MGs) show some unique properties [1–3]; due to their low coercivity and high permeability, combined with a high electrical resistivity which is helpful for reducing eddy current losses, soft magnetic MGs are widely used in laminated transformer cores [4–6]. Besides, due to the relatively cheap raw materials, acceptable glass-forming ability (GFA), good corrosion resistance, and high elastic strength, they are promising as structural engineering materials [6–9]. During the past decades, many Fe-based MG systems have been developed. One family of large interest is the Fe–Mo–C–B amorphous steels [8–10]. Thermal characterization on doping concentration of Cr in Fe–Mo–C–B MGs was investigated in Ref. [11]. Detailed phase evolution during the crystallization process was characterized using electron diffraction by Duarte [3, 12], and the effect of doping with Nb on the GFA and mechanical properties was investigated in Ref. [13].

Room temperature uniaxial compression of Fe₄₆Cr₁₅Mo₁₄C₁₅B₆Nb₄ bulk metallic glass (BMG) with diameter of 2 mm suggests that there is no macro-plastic deformation in this composition at a deformation rate of 10^{-4} s^{-1} , as deduced from the microstructure of the fracture surface [13, 14]. Actually, not only in this specific MG, a big overall challenge on the design of MGs as structural materials is the control of their fracture mechanism [15, 16]. Another topic of great interest is the investigation of the crystallization kinetics in MGs [17–19], both for characterizing the stability of the glass and for the production of in situ composites with improved mechanical properties. As to the monolithic MGs, since deformation mechanisms involved in crystalline materials such as dislocation, twinning, and sliding between grain boundaries are not possible in amorphous materials, other mechanisms

✉ Chaoren Liu
chaorenliu@gmail.com

¹ Departament de Física, EETAC, Universitat Politècnica de Catalunya - BarcelonaTech, 08860 Castelldefels, Spain

² Departament de Física, ESAB, Universitat Politècnica de Catalunya - BarcelonaTech, 08860 Castelldefels, Spain

have to be introduced for the glassy systems [20]. Argon's concept of shear transformation zones [21] and Spaepen's free volume theory [22] are often employed to describe the microscopic deformation mechanism for steady state inhomogeneous flow in MGs.

The understanding of the mechanical behavior of metallic glasses has also to consider the fact that glasses are, by definition, non-ergodic materials. Thus, the atomic configuration is continuously evolving toward a lower energy configuration. The kinetics of this process is controlled by temperature. At low temperatures, the timescale of the structural evolution is longer than any observable scale, but it shortens at increasing temperatures. Below the glass transition, still in the solid state, the thermal excitation allows the atoms to find lower energy states in an irreversible process termed structural relaxation or physical aging. At temperatures near T_g , this process is expected to be linked to the primary or α relaxation. This is the same collective atomic movement governing the viscous flow of the liquid phase. At lower temperatures, more subtle atomic movements like the secondary or β relaxation are thought to govern structural relaxation.

The terminology of secondary relaxation is often related to mechanical relaxation. Mechanical relaxation dynamics is a time-dependent response behavior under stress or strain stimuli. Mechanical spectroscopy, by applying a periodic excitation and analyzing the phase lag between the stimuli and response, has been proven to be an effective method for exploring the dynamics of glassy systems [23–27]. The relaxation dynamics in metallic glasses has attracted great attention recently [1, 24, 28–31]. There is a great interest in interpreting the mechanical properties in terms of relaxation events and the effect of structural relaxation on the mechanical properties [32], as well as to understand the microscopic nature of these relaxation events [33].

Experimentally, mechanical spectroscopy is performed either by varying the testing frequencies under isothermal conditions or by varying temperature and setting a constant frequency [34]. In the former case, the frequency window is normally between 0.01 and 100 Hz due to experimental constraints. In the latter, the temperature window is normally between room and glass transition temperatures. In the case of polymers, secondary relaxation is often observed in the continuous heating mode, although it might have different origin in different materials. For both primary and secondary relaxations, the response as function of frequency and relaxation time can be fitted with the Havriliak–Negami (HN) function [27]:

$$\chi(\omega) = \frac{1}{[1 + (i\omega\tau)^{\alpha}]^{\gamma}} \quad (1)$$

Besides HN function, the response function is sometimes described by the less parameterized Cole–Davison

(CD) or Cole–Cole (CC) functions (where exponents $\alpha = 1$ or $\gamma = 1$, respectively). The HN approach is quite successful in the analysis of α relaxation; it was first employed as interpretation of the dielectric response in polymers. It is in general accepted that the glass transition is related to the slowdown of α relaxation and the corresponding arrest of the liquid viscous flow. Below the glass transition temperature, the relaxation time of α relaxation is longer than the testing time, thus α relaxation can be viewed as frozen. However, well below the glass transition there are still active relaxation processes which could be detected by dielectric or mechanical spectroscopy [34]. In the case of polymers, these processes might involve the movement of atoms on the side chain, and they are normally called β relaxation. In the case of metallic glasses, probably due to the contribution of deformation units with lower activation energies among the whole distribution, β relaxation is mostly manifested on the mechanical spectroscopy $E''(\omega, T)$ behavior [28, 29]. The β relaxation in metallic glasses is ascribed as Johari–Goldstein β relaxation, though the concept originated from translational motions of molecules [35, 36] is difficult to apply to MGs where the atomic movement is most likely individual. Besides the Johari–Goldstein β relaxation model, the dynamical concentration excitation model in which relaxation is treated as a cooperative restructuration of atomic configurations is also employed to understand the non-diffusive nature of these secondary relaxation processes [37].

Due to the softening behavior as temperature is increased, MGs start to flow below the glass transition temperature. This opens a way of forming the material into complex shapes in a single step. In such cases, relaxation dynamics and viscosity are key factors for designing the processing conditions. For instance, processes like fiber drawing or glass blowing could be performed at temperatures where viscosity reaches 10^8 Pa s. Other techniques like annealing and bubble removal, as employed in oxide glasses, are also closely related to the viscosity behavior. Thus, the knowledge of the mechanical relaxation behavior of MGs is critical to define their technological potential. Besides, it does not only play an important role in technical aspects; as claimed by Gupta [38], the isostructural viscosity is also of crucial importance in testing in detail the proposed models of the glass transition theory.

Experimentally, the shear viscosity can be determined under tensile deformation mode by

$$\eta = \frac{\sigma}{3\dot{\epsilon}} \quad (2)$$

where σ is the tensile stress and $\dot{\epsilon}$ is the shear strain rate. The temperature-dependent viscosity is obtained by deforming at different temperatures. In the framework of this methodology, activation energy of viscous flow could

be determined. Close to glass transition temperature, the fragility parameter is defined as [27, 39]:

$$m = \left. \frac{d \log \eta}{dT_g/T} \right|_{T=T_g} = \frac{E_\alpha}{RT_g \ln 10} \quad (3)$$

where E_α is the apparent activation energy of viscous flow in the liquid state at the glass transition region. In the glassy state, if the system is in a non-isoconfigurational state, the change of state due to structural relaxation influences the properties of the glass. In metallic glasses, aging is generally seen as a release of excess free volume. Rejuvenation, introduced by either ion irradiation, surface blasting (shot-peening), severe deformation, or cryogenic thermal cycling techniques [40], introduces free volume to the system. Both structural relaxation and rejuvenation have large effect on physical as well as mechanical properties. Interestingly, secondary relaxation seems to be connected to the properties of the glass both at low temperatures and close to the glass transition. Wang's work on La–Ni–Y MGs shows that the activation energy of the secondary relaxation is comparable to the activation energy of shear transformation zones [41, 42]. It is suggested that they may share the same origin. If this is true, the presence of secondary relaxation might be helpful to improve the mechanical properties of metallic glasses at elevated or room temperature, according to the activation energy distribution of the activation centers involved in the process [42–44]. The activation of shear transformation zones may lead to plasticity on the small scale or in constrained deformation modes like bending [45].

In this work, the mechanical relaxation dynamics of a Fe₅₅Cr₁₀Mo₁₄C₁₅B₆ stainless MG is explored through mechanical spectroscopy. The β relaxation is observed by mechanical spectroscopy and the activation energy is analyzed in the framework of standard anelastic solids. Viscosity information is obtained from elongation measurements. The effect of structural relaxation on mechanical spectroscopy as well as viscosity is explored. Finally, structural relaxation manifested on enthalpy change and the corresponding activation energy spectrum are also explored by calorimetry.

Experimental method

Metallic glass ribbons with nominal composition Fe₅₅Cr₁₀Mo₁₄C₁₅B₆ were obtained as described in Ref. [11]. Mechanical spectroscopy of the ribbons was performed in tension mode in a TA Q800 Dynamic mechanical analyzer (DMA). The length of the ribbons was around 15 mm. Multifrequency tests ranging between 0.1 and 50 Hz were performed at a constant heating rate of 2 K min⁻¹. A sinusoidal strain of 2 μ m amplitude was applied on the

samples, preloaded with a static force of 1 N. Differential scanning calorimetry (DSC) was performed at a heating rate of 20 K min⁻¹ using a Netzsch 403 F3 equipment. As described by Chen [46], the difference between the heat flux of the as-quenched state and relaxed state was employed to build the activation energy spectrum. The relaxed state was obtained by heating the sample at a heating rate of 20 K min⁻¹ up to 813 K, above the glass transition temperature, and cooling back to room temperature with the same controlled cooling rate. By this thermal pre-treatment, it is expected that the structural relaxation is not significant during posterior heating ramps at the same rate and, therefore, the system can be considered in an isoconfigurational state until reaching glass transition.

Results and discussion

Thermal characterization

DSC results of Fe₅₅Cr₁₀Mo₁₄C₁₅B₆, displayed in Fig. 1, show that the glass transition starts at 790 K when heating at a rate of 20 K min⁻¹. The crystallization process is a multistep process, as it is commonly observed in many metallic glasses [47]. The first crystallization step starts at 835 K, and the second crystallization process is entangled with the first crystallization process having its crystallization peak at 878 K. The third crystallization peak appears at 937 K. The characterization of the crystallization process was detailed in Refs. [11, 48].

Mechanical relaxation

The typical multifrequency mechanical spectroscopy results on as-quenched Fe₅₅Cr₁₀Mo₁₄C₁₅B₆ MG are shown

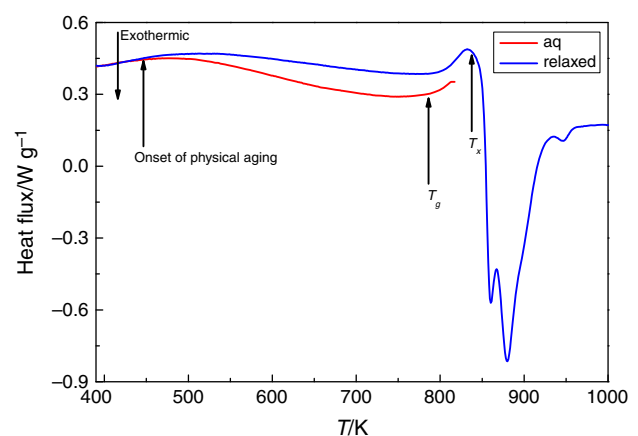


Fig. 1 DSC curves of Fe₅₅Cr₁₀Mo₁₄C₁₅B₆ MG applying a heating rate of 20 K min⁻¹. As-quenched ribbons (dark red line) compared with pre-annealed relaxed ribbons (blue line). (Color figure online)

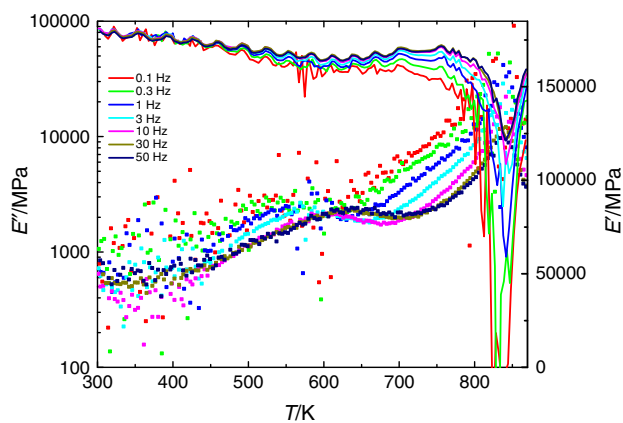


Fig. 2 Storage (*solid lines*) and loss (*dots*) moduli obtained by mechanical spectroscopy of as-quenched $\text{Fe}_{55}\text{Cr}_{10}\text{Mo}_{14}\text{C}_{15}\text{B}_6$ MG under frequencies varying from 0.1 to 50 Hz. There is obvious secondary relaxation at around 500 K. The peak at 820 K is not the complete α relaxation, but it is cut by crystallization

in Fig. 2. From 450 K, the loss modulus starts to increase and shows a distinct peak between 550 K and 630 K as the test frequency increases from 0.1 to 50 Hz. This distinguishable peak is also reported in La–Ni–Y MGs, where is normally referred as β relaxation. At even higher temperatures, the loss modulus increases continuously with temperature until it is cut by crystallization and starts to decrease. This behavior of a separate low temperature peak on the $E''(T)$ profile is not general in MGs. In $\text{Pd}_{42.5}\text{Ni}_{7.5}\text{Cu}_{30}\text{P}_{20}$, for instance, the loss modulus shows a prominent shoulder, but it increases continuously with temperature and both $\text{Cu}_{46}\text{Zr}_{46}\text{Al}_8$ and $\text{Mg}_{65}\text{Cu}_{25}\text{Y}_{10}$, also studied in the same way, showing just an excess wing of the primary relaxation instead. In $\text{Cu}_{46}\text{Zr}_{46}\text{Al}_8$ MG, the experimental loss modulus was simulated with only a primary relaxation process described by the CC function with a main relaxation time following a Vogel–Fulcher–Tammann (VFT) behavior above T_g and an Adams–Gibbs–Vogel (AGV) behavior below it [49]. This CC fitting was found to be also applicable to the $\text{Mg}_{65}\text{Cu}_{25}\text{Y}_{10}$ MG where the $E''(\omega, T)$ of the as-quenched glass showed a shoulder-like behavior attributed to in situ physical aging during the DMA measurement [23]. In this latter case, the induction of physical aging by annealing treatments eliminated the secondary peak of the loss modulus.

In order to describe the low temperature peak, here we will assume that it is a thermal activated process whose relaxation time dependence of temperature follows an Arrhenius relationship with the dynamic equation of a standard anelastic solid. The anelastic event can be analyzed in the framework of the Debye equation [50]:

$$\ln(\omega_{\text{peak}}\tau) = 0 = \ln(\omega_{\text{peak}}\tau_0) + \left(\frac{E}{k_B}\right)\left(\frac{1}{T}\right) \quad (4)$$

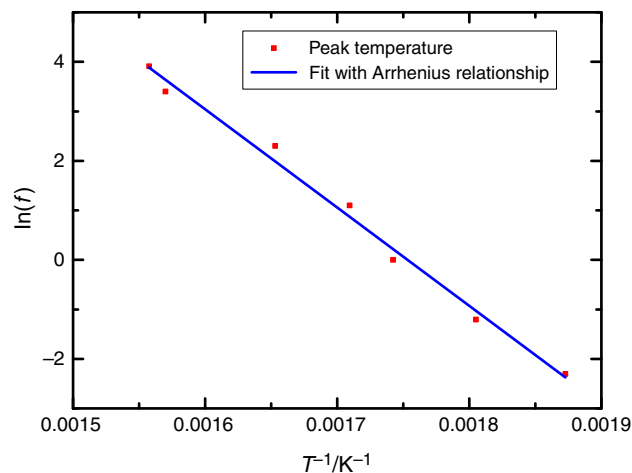


Fig. 3 Peak temperature dependence of testing frequency showing secondary relaxation in as-quenched $\text{Fe}_{55}\text{Cr}_{10}\text{Mo}_{14}\text{C}_{15}\text{B}_6$ MG. $E_a = 165 \text{ kJ mol}^{-1}$

$$\ln\left(\frac{\omega_{\text{peak}2}}{\omega_{\text{peak}1}}\right) = \left(\frac{E}{k_B}\right)\left(\frac{1}{T_1} - \frac{1}{T_2}\right) \quad (5)$$

Figure 3 displays $\ln(f_{\text{peak}})$, $f_{\text{peak}} = \omega_{\text{peak}}/2\pi$, versus $1/T_{\text{peak}}$ for the as-quenched sample showing the validity of the proposed model. The activation energy of the relaxation can be determined from the dependence of the peak temperature on the testing frequency, according to Eq. 5. For the as-quenched state, the fitted activation energy is 165 kJ mol^{-1} and the pre-exponential factor is $1.3 \times 10^{15} \text{ s}^{-1}$. According to the relationship $E_\beta = 26RT_g$ [42, 51, 52], widely used in the literature, taking $T_g = 790 \text{ K}$ as obtained by calorimetry, the activation energy of the Johari–Goldstein relaxation would be around 171 kJ mol^{-1} . The activation energy of the low temperature relaxation determined here is thus close to the value expected for Johari–Goldstein relaxations in metallic glasses; however, with only the activation energy it is difficult to tell whether the secondary relaxation is a JG relaxation or not. The ω_0 obtained is on the order of 10^{15} s^{-1} , which is close to Debye frequency, and this is within the order of magnitude expected for an atomic jump process.

Our previous work shows that structural relaxation affects the bulk and loss modulus of Cu–Zr–Al and Mg–Cu–Y MGs [23, 27, 49]. Actually, the effect of physical aging and rejuvenation on mechanical relaxation is a topic of great interest, recently studied also in Pd–Ni–Cu–P [53] as well as Ti–Zr–Ni–Cu–Be [54] MGs. In this work, structural relaxation of $\text{Fe}_{55}\text{Cr}_{10}\text{Mo}_{14}\text{C}_{15}\text{B}_6$ in isothermal conditions was performed, and mechanical spectroscopy of the relaxed samples was explored. The mechanical

spectroscopy of the samples relaxed at 723 and 773 K for 30 min is displayed in Fig. 4, showing the effect of structural relaxation. In the case of as-quenched sample, the storage modulus shows an increase at elevated temperatures. This behavior is attributed to the physical aging, as also perceived in Mg–Cu–Y MG [23].

The activation energy of the β relaxation of relaxed samples was calculated by using Eqs. 4 and 5. In the case of the sample relaxed at 723 K, the activation energy is found 152 kJ mol^{-1} with pre-exponential factor of $3.6 \times 10^{13} \text{ s}^{-1}$, while the sample relaxed at 773 K shows an activation energy of 181 kJ mol^{-1} with pre-exponential factor of $7 \times 10^{15} \text{ s}^{-1}$. A similar activation energy is obtained by DMA in La–Ni–Al MGs as well as by NMR in Zr–Ti–Cu–Ni–Be MG [55]. It has been suggested that these processes are dominated by the slow atomic motion induced by the smallest atoms [44]. The activation energy of β relaxation is comparable with the activation energy of the shear transformation zones, and it is believed that enhancing β relaxation might be beneficial for mechanical properties of MGs like plasticity and toughness [56–58]. Our results here, showing a distinctive secondary relaxation, suggest that when the β relaxation gets activated at elevated temperature plasticity may get improved in this alloy. Since chemical composition influences both the intensity as well as peak position of the β relaxation [30], further research might include systematic work reducing the activation energy of β relaxation with the aim of improving toughness, as achieved in La-based MG system with notable β relaxations [43].

In situations when the peak is not distinguishable, the temperatures at which the material shows the same value of

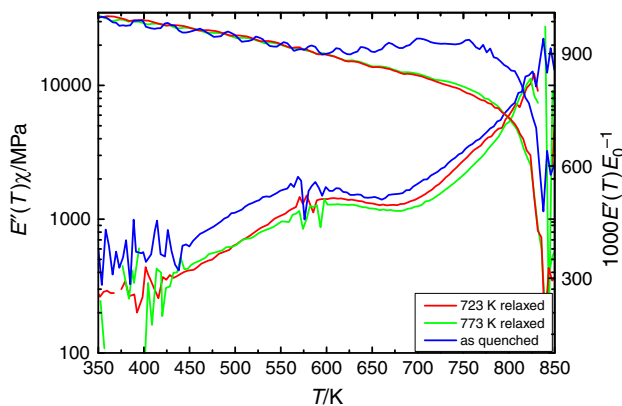


Fig. 4 Effect of structural relaxation on mechanical relaxation. Loss modulus measured at 3 Hz and at a heating rate of 2 K min^{-1} . Storage modulus $E'(T)$ profiles are normalized with $E'_0 = E'(300 \text{ K})$, which are 140, 147, and 180 GPa for the 723 K relaxed, 773 K relaxed, and as-quenched state, respectively. $E''(T)$ of the 773 K relaxed and as-quenched samples is rescaled to sample relaxed at 723 K by using a corresponding coefficient $E'_0(\text{sample})/E'_0(\text{relaxed at } 723 \text{ K})$

the loss modulus are employed to calculate the activation energy. When a fixed loss modulus value of 1500 MPa is chosen, the activation energy computed for this alloy is found to be 99 kJ mol^{-1} , with a pre-exponential factor of $4.9 \times 10^{10} \text{ s}^{-1}$. The activation energy fitted with a fixed loss modulus value is lower than that fitted from the peak position. This indicates that, as expected, the secondary peak is originated from a distribution of processes with a corresponding distribution of activation energies. Although an average relaxation time and activation energy may be calculated, the fastest processes of the distribution (which have the lowest activation energies) get activated at lower temperatures.

At higher temperatures, close to T_g , a peak is observed in the loss modulus. The peak temperature shifts to higher values when the frequency is increased. This increase of loss modulus can be ascribed to α relaxation involving the activation of collective movement. The peak here is cut by the crystallization process which further decreases the loss modulus at higher temperature. Using a fixed loss modulus value of 9200 MPa, the temperatures corresponding to each frequency are determined. Using Eq. 5, the activation of this α process is calculated to be 461 kJ mol^{-1} . However, as illustrated above in the case of the anelastic event, the activation energy obtained by a fixed value is lower than that obtained fitting from peak temperatures; the value of 461 kJ mol^{-1} might thus be an underestimation of the actual α relaxation activation energy. Using Eq. 2, this apparent activation energy of the viscous flow in the glass transition region gives a fragility parameter of $m = 30$, which is quite low for this metallic glass. Thus, we will have to consider an alternative way to determine the proper value of fragility (Fig. 5).

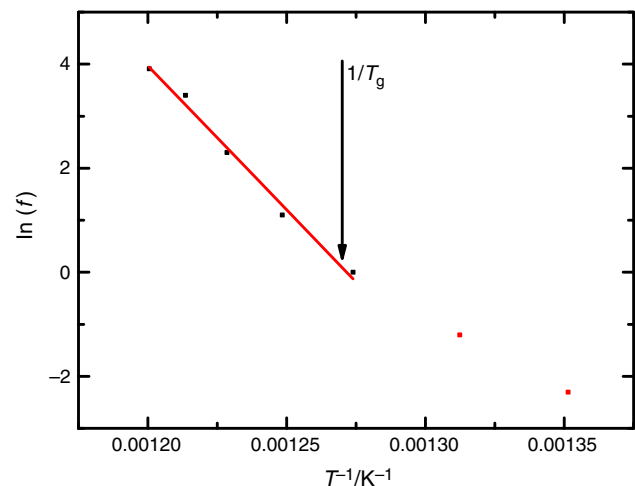


Fig. 5 α relaxation analyzed by Eq. 4. Temperatures are chosen as loss modulus reaches a fixed value of 9200 MPa at each frequency. Red line is the fit to an Arrhenius behavior with activation energy of 461 kJ mol^{-1} . Below T_g , the system is in a non-equilibrium state and the behavior deviates from the expected equilibrated liquid state. (Color figure online)

The temperature-dependent viscosity is of great interest [59, 60]. The viscosity during mechanical spectroscopy measurement can be obtained as detailed in Refs. [61, 62]. The dependence of viscosity on temperature for this alloy is illustrated in Fig. 6. Viscosity decreases with increasing temperature. T_g , determined where viscosity reaches 10^{12} Pa s, is around 788 K. This is quite close to the 790 K obtained by DSC measurement under a heating rate of 20 K min^{-1} . At temperatures higher than 837 K, viscosity increases with temperature; this increase on viscosity is related to crystallization. This agrees with the enthalpy measurements that showed $T_x = 835 \text{ K}$. In the valid temperature window, from room temperature to crystallization temperature, viscosity decreases from 10^{14} to 10^{10} Pa s. This suggests that this MG family cannot be blown into complex shapes due to the fact that viscosity values of $\sim 10^6$ Pa s are needed for proper shape forming.

The temperature-dependent viscosity follows an Arrhenius relationship below T_g . In the case of the as-quenched state, the apparent activation energy is found to be 180 kJ mol^{-1} , which is slightly larger than the 165 kJ mol^{-1} obtained from fitting the secondary relaxation peak of the loss modulus. The slopes of the viscosity versus $1/T$ curves of the samples relaxed at 723 and 773 K are higher than that the one shown by the as-quenched ribbons, in agreement with the expected increase of the activation energy for sub- T_g viscous flow because of physical aging. Above T_g , the temperature-dependent viscosity can be described by a VFT function or also by a local Arrhenius behavior. Fitting with Arrhenius relationship leads to $E_x = 746 \text{ kJ mol}^{-1}$. This high apparent

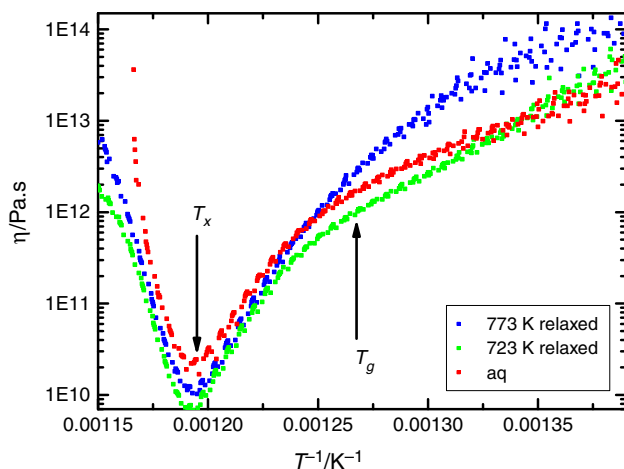


Fig. 6 Viscosity of the $\text{Fe}_{55}\text{Cr}_{10}\text{Mo}_{14}\text{C}_{15}\text{B}_6$ metallic glass obtained from $\eta = \sigma/3 \dot{\epsilon}$. The viscosity can be described by an Arrhenius behavior under T_g , while it can be fitted with an Arrhenius behavior above T_g . Further heating above the crystallization temperature would increase viscosity. Measurements were performed at a heating rate of 2 K min^{-1}

activation energy for α relaxation might be attributed to the dependence of the shear modulus on temperature [28]. With Eq. 2, the corresponding fragility parameter results to be $m = 49$. This fragility parameter agrees with the reported values in similar compositions [63].

Structural relaxation explored by calorimetry

The DSC curves of $\text{Fe}_{55}\text{Cr}_{10}\text{Mo}_{14}\text{C}_{15}\text{B}_6$ as-quenched and relaxed samples, presented in Fig. 1, show that structural relaxation starts around 500 K. In order to gain a deeper insight in the distribution of activation energies, a controlled physical aging was performed in the DSC by performing successive isothermal annealing processes at increasing temperatures. The recorded heat flow is depicted in Fig. 7. At a given temperature, after the characteristic relaxation time, the structural relaxation process is finished and the heat capacity retains a stable value. When heating to higher temperature, an additional release of heat is observed. This behavior is continuous until the glass transition region, where the system reaches the configuration of the supercooled liquid state which is in internal equilibrium and there is no more structural relaxation.

Recently, the idea of activation energy spectrum (AES) of structural relaxation has regained great interest because of its relation with the plasticity of MGs [64, 65]. The difference between the heat flow of the as-quenched and relaxed states, $\Delta W(T)$, can be used to construct the AES as detailed in Refs. [66, 67] with the relationship between the temperature and the activation energy in the form of $E = aT$, where a is between 0.002 and 0.003 eV K^{-1} depending on the heating rate [68, 69]. Chen assumed

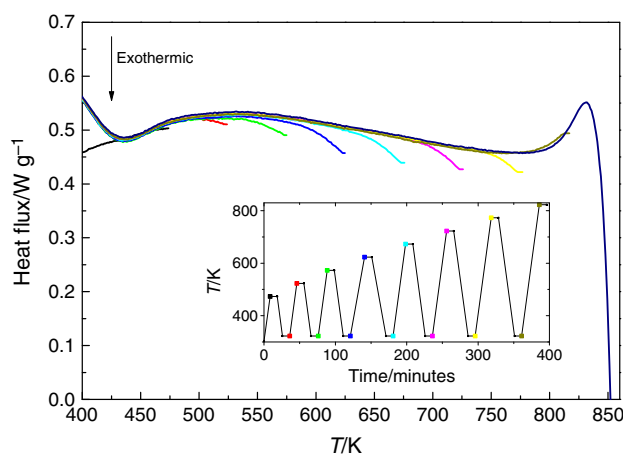


Fig. 7 DSC of $\text{Fe}_{55}\text{Cr}_{10}\text{Mo}_{14}\text{C}_{15}\text{B}_6$ MG isothermally annealed at increasing temperatures, according to the controlled heating and cooling protocol explained in the inset figure. The heat flux curves in the figure were obtained from the heating portions in the temperature history, and isothermal and cooling steps are not displayed

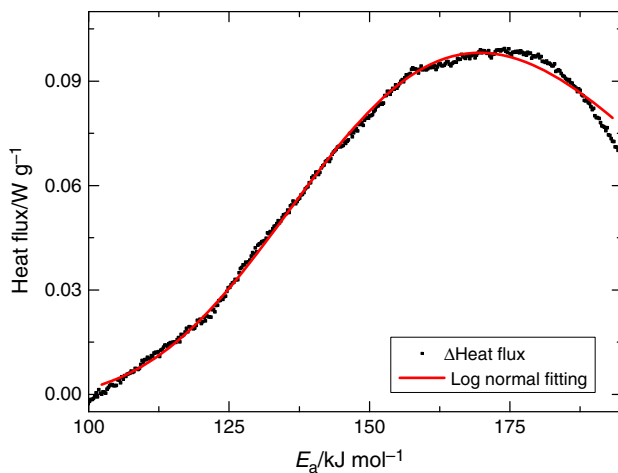


Fig. 8 Temperature-dependent physical aging behavior of Fe₅₅Cr₁₀Mo₁₄C₁₅B₆. The *black points* give the difference of the heat flow between the as-quenched and relaxed states. The *red line* shows a fit to a lognormal distribution. (Color figure online)

$a = 0.0025 \text{ eV K}^{-1} = 0.241 \text{ kJ mol}^{-1} \text{ K}^{-1}$ for a heating rate of 20 K min^{-1} [46]. This methodology of AES is applied as described by Chen [46] and Khonik [68, 69], the latter suggests that a continuous distribution of activation energies is a typical feature of structural relaxation in MGs and that it is directly related to the shear modulus change between relaxed and as-quenched samples [68]. The difference between heat flux of the as-quenched and the relaxed states as function of $E = aT$ is shown in Fig. 8.

Unlike Pd–Ni–P MG where there are two events with separate activation energies [64, 65], the Fe–Cr–Mo–C–B MG has only one event with a wide activation energy distribution; the $\Delta W(E)$ is proportional to the AES and can be fitted to a lognormal distribution

$$y = y_0 + \frac{A}{\sqrt{2\pi}wE} \exp\left(-\frac{\ln^2(E/E_c)}{2w^2}\right) \quad (6)$$

with fitting parameters $y_0 = -0.0017(\pm 0.0004)$, $E_c = 176(\pm 1)$, $w = 0.202(\pm 0.001)$, and $A = 8.782(\pm 0.037)$. Here, the E_c is the most probable activation energy and w is a parameter determining the distribution shape and could be regarded as a broadening parameter. This experimental lognormal distribution agrees with Jiao's assumption used in fitting the stress relaxation of Pd₄₀Ni₁₀Cu₃₀P₂₀ glass [70].

The value of E_c is close to the Johari–Goldstein β relaxation activation energy of 171 kJ mol^{-1} obtained using the empirical relationship $E_\beta = 26RT_g$. The similar activation energies of structural relaxation, secondary relaxation from mechanical spectroscopy and the estimated Johari–Goldstein β relaxation suggest them as sharing the

same microscopic origin. The calorimetric measurements suggest that for each temperature the structural relaxation might be finished after a certain period. However, mechanical relaxation results show that β relaxation is still perceived in samples after relaxation at 773 K for 30 min . This implies that the atomic movements responsible of the anelastic secondary relaxation are still present in the well-relaxed glass, there not producing any change of state. The similar activation energies found from calorimetric and mechanical spectroscopy measurements indicate that these intrinsic anelastic events of the glass state are also the vehicle of physical aging, driving the system toward more stable configurations.

Conclusions

In this work, the relaxation dynamics of a Fe₅₅Cr₁₀Mo₁₄C₁₅B₆ stainless amorphous steel is explored by mechanical relaxation and calorimetry. The mechanical response in the temperature region below the glass transition can be modeled as a thermal activated secondary relaxation. The activation energy is calculated under the standard anelastic solid model obtaining an activation energy of 165 kJ mol^{-1} . The increase of the loss modulus at higher temperatures, around the glass transition region, corresponds to the collective movement responsible of the α relaxation. The sub- T_g structural relaxation is also explored by successive isothermal annealing at increasing temperatures. The activation energy spectrum of enthalpy relaxation is obtained from the difference between the heat flux of as-quenched and relaxed samples. The activation energy spectrum shows a lognormal distribution with a peak at 176 kJ mol^{-1} . The measurements show similar activation energy values for secondary relaxation, structural relaxation, and the estimated Johari–Goldstein β process. This suggests the microscopic movements generating the anelastic reversible mechanical relaxation in a well-relaxed state are very similar to the ones governing the change of state during physical aging. The very complete characterization of the relaxation dynamics of Fe₅₅Cr₁₀Mo₁₄C₁₅B₆ MG presented here is useful for determining at which temperatures the microscopic events governing sub- T_g plastic deformation become activated. In this way, this work is expected to help devising the optimal treatment temperatures for mechanization and shape forming of this type of materials.

Acknowledgments This work was funded by MINECO, Grant FIS2014-54734-P, and Generalitat de Catalunya, Grant 2014SGR00581. C. Liu is supported by Generalitat de Catalunya, FI Grant 2012FI_B00237.

References

- Amir A, Oreg Y, Imry Y. On relaxations and aging of various glasses. *Proc Natl Acad Sci*. 2012;109:1850–5.
- Herzer G. Modern soft magnets: amorphous and nanocrystalline materials. *Acta Mater*. 2013;61:718–34.
- Duarte MJ, Klemm J, Klemm SO, Mayrhofer KJJ, Stratmann M, Borodin S, Romero AH, Madinehei M, Crespo D, Serrano J, Gerstl SSA, Choi PP, Raabe D, Renner FU. Element-resolved corrosion analysis of stainless-type glass-forming steels. *Science*. 2013;341:372.
- Inoue A. Bulk amorphous alloys with soft and hard magnetic properties. *Mater Sci Eng, A*. 1997;226–228:357–63.
- Inoue A, Koshiba H, Zhang T, Makino A. Wide supercooled liquid region and soft magnetic properties of Fe₅₆Co₇Ni₇Zr₀₋₁₀Nb(or Ta)₀₋₁₀B₂₀ amorphous alloys. *J Appl Phys*. 1998;83:1967–74.
- Suryanarayana C, Inoue A. Iron-based bulk metallic glasses. *Int Mater Rev*. 2013;58:131–66.
- Gu XJ, Poon SJ, Shiflet GJ. Mechanical properties of iron-based bulk metallic glasses. *J Mater Res*. 2007;22:344–51.
- Gu XJ, Poon SJ, Shiflet GJ, Widom M. Ductility improvement of amorphous steels: roles of shear modulus and electronic structure. *Acta Mater*. 2008;56:88–94.
- Gu XJ, McDermott AG, Poon SJ, Shiflet GJ. Critical Poisson's ratio for plasticity in Fe–Mo–C–B–Ln bulk amorphous steel. *Appl Phys Lett*. 2006;88:211905.
- Lu ZP, Liu CT, Thompson JR, Porter WD. Structural amorphous steels. *Phys Rev Lett*. 2004;92:245503.
- Madinehei M, Bruna P, Duarte MJ, Pineda E, Klemm J, Renner FU. Glass-formation and corrosion properties of Fe–Cr–Mo–C–B glassy ribbons with low Cr content. *J Alloys Compd*. 2014;615:S128–31.
- Duarte MJ, Kostka A, Jimenez JA, Choi P, Klemm J, Crespo D, Raabe D, Renner FU. Crystallization, phase evolution and corrosion of Fe-based metallic glasses: an atomic-scale structural and chemical characterization study. *Acta Mater*. 2014;71:20–30.
- Zhai F, Pineda E, Duarte MJ, Crespo D. Role of Nb in glass formation of Fe–Cr–Mo–C–B–Nb BMGs. *J Alloys Compd*. 2014;604:157–63.
- Zhai F. Investigation on the synthesis and characterization of amorphous steels. Ph.D. Thesis. Universitat Politècnica de Catalunya. 2015.
- Chen M. Mechanical behavior of metallic glasses: microscopic understanding of strength and ductility. *Annu Rev Mater Res*. 2008;38:445–69.
- Ashby MF, Greer AL. Metallic glasses as structural materials. *Scr Mater*. 2006;54:321–6.
- Gong P, Yao K, Zhao S. Cu alloying effect on crystallization kinetics of Ti₄₁Zr₅Be₂₈Fe₆ bulk metallic glass. *J Therm Anal Calorim*. 2015;121:697–704.
- Lu XC, Li HY. Kinetics of non-isothermal crystallization in Cu₅₀Zr₄₃Al₇ and (Cu₅₀Zr₄₃Al₇)₉₅Be₅ metallic glasses. *J Therm Anal Calorim*. 2014;115:1089–97.
- Wu J, Pan Y, Pi J. On non-isothermal kinetics of two Cu based bulk metallic glasses. *J Therm Anal Calorim*. 2014;115:267–74.
- Schuh CA, Hufnagel TC, Ramamurty U. Mechanical behavior of amorphous alloys. *Acta Mater*. 2007;55:4067–109.
- Argon AS. Plastic deformation in metallic glasses. *Acta Metall*. 1979;27:47–58.
- Spaepen FA. Mechanism for steady state inhomogeneous flow in metallic glasses. *Acta Metall*. 1976;25:407–15.
- Pineda E, Bruna P, Ruta B, Gonzalez-Silveira M, Crespo D. Relaxation of rapidly quenched metallic glasses: effect of the relaxation state on the slow low temperature dynamics. *Acta Mater*. 2013;61:3002–11.
- Qiao JC, Pelletier JM. Dynamic mechanical relaxation in bulk metallic glasses: a review. *J Mater Sci Technol*. 2014;30:523–45.
- Yu HB, Wang WH, Samwer K. The beta relaxation in metallic glasses: an overview. *Mater Today*. 2013;16:183–91.
- Wang WH, Wen P, Liu XF. The excess wing of bulk metallic glass forming liquids. *J Non Cryst Solids*. 2006;352:5103–9.
- Liu C, Pineda E, Crespo D. Mechanical relaxation of metallic glasses: an overview of experimental data and theoretical models. *Metals*. 2015;5:1073–111.
- Ju JD, Atzmon MA. Comprehensive atomistic analysis of the experimental dynamic-mechanical response of a metallic glass. *Acta Mater*. 2014;74:183–8.
- Ju JD, Atzmon MA. Atomistic interpretation of the dynamic response of glasses. *MRS Commun*. 2014;4:63–6.
- Yu HB, Samwer K, Wang WH, Bai HY. Chemical influence on β -relaxations and the formation of molecule-like metallic glasses. *Nat Commun*. 2013;4:2204.
- Yu H, Wang W, Bai H, Samwer K. The β relaxation in metallic glasses. *Nat Sci Rev*. 2014;1:429–61.
- Kahl A, Koeppe T, Bedorf D, Richert R, Lind ML, Demetriou MD, Johnson WL, Arnold W, Samwer K. Dynamical and quasi-static structural relaxation paths in Pd₄₀Ni₄₀P₂₀ glass. *Appl Phys Lett*. 2009;95:201903.
- Wang Z, Wen P, Huo LS, Bai HY, Wang WH. Signature of viscous flow units in apparent elastic regime of metallic glasses. *Appl Phys Lett*. 2012;101:121906.
- Rao KJ. Structural chemistry of glasses. Amsterdam: Elsevier; 2002.
- Hu L, Yue Y. Secondary relaxation in metallic glass formers: its correlation with the genuine Johari–Goldstein relaxation. *J Phys Chem C*. 2009;113:15001–6.
- Johari GP. Localized molecular motions of beta-relaxation and its energy landscape. *J Non Cryst Solids*. 2002;307–310:317–25.
- Egorushkin VE, Mel'nikova NV. Structural relaxation in amorphous metallic alloys. *Zh Eksp Teor Fiz*. 1993;103:555.
- Gupta PK, Heuer A. Physics of the iso-structural viscosity. *J Non Cryst Solids*. 2012;358:3551–8.
- Angell C. Formation of glasses from liquids and biopolymers. *Science*. 1995;267:1924–35.
- Ketov SV, Sun YH, Nachum S, Lu Z, Checchi A, Beraldin AR, Bai HY, Wang WH, Louzguine-Luzgin DV, Carpenter MA, Greer AL. Rejuvenation of metallic glasses by non-affine thermal strain. *Nature*. 2015;524:200–3.
- Liu ST, Wang Z, Peng HL, Yu HB, Wang WH. The activation energy and volume of flow units of metallic glasses. *Scr Mater*. 2012;67:9–12.
- Yu HB, Wang WH, Bai HY, Wu Y, Chen MW. Relating activation of shear transformation zones to β relaxations in metallic glasses. *Phys Rev B*. 2010;81:220201.
- Yu HB, Shen X, Wang Z, Gu L, Wang WH, Bai HY. Tensile plasticity in metallic glasses with pronounced β relaxations. *Phys Rev Lett*. 2012;108:015504.
- Yu HB, Samwer K, Wu Y, Wang WH. Correlation between beta relaxation and self-diffusion of the smallest constituting atoms in metallic glasses. *Phys Rev Lett*. 2012;109:095508.
- Xi XK, Zhao DQ, Pan MX, Wang WH, Wu Y, Lewandowski JJ. Fracture of brittle metallic glasses: brittleness or plasticity. *Phys Rev Lett*. 2005;94:125510.
- Chen HS, Coleman E. Structure relaxation spectrum of metallic glasses. *Appl Phys Lett*. 1976;28:245–7.
- Sonal RP, Supriya K, Ashmi TP, Arun P. Non-isothermal crystallization kinetics of Zr₅₂Cu₁₈Ni₁₄Al₁₀Ti₆ metallic glass. *J Therm Anal Calorim*. 2015;. doi:10.1007/s10973-015-4979-0.
- Madinehei M. Improvement of corrosion and mechanical properties of amorphous steels by microalloying and nanocrystallization. Ph.D. Thesis. Universitat Politècnica de Catalunya; 2015.

49. Liu C, Pineda E, Crespo D. Characterization of mechanical relaxation in a Cu–Zr–Al metallic glass. *J Alloys Compd.* 2014;643:s17–21.
50. Nowick AS, Berry BS. Anelastic relaxation in crystalline solids. London: Academic press; 1972.
51. Hu L, Zhou C, Zhang C, Yue Y. Thermodynamic anomaly of the sub- T_g relaxation in hyperquenched metallic glasses. *J Chem Phys.* 2013;138:174508.
52. Liu YH, Fujita T, Aji DPB, Matsuura M, Chen MW. Structural origins of Johari–Goldstein relaxation in a metallic glass. *Nat Commun.* 2014;5:3238.
53. Qiao JC, Pelletier J, Casalini R. *J Phys Chem B.* 2013;117(13658–1366):6.
54. Qiao JC, Pelletier JM, Kou HC, Zhou X. Modification of atomic mobility in a Ti-based bulk metallic glass by plastic deformation or thermal annealing. *Intermetallics.* 2012;28:128–37.
55. Yuan CC, Xiang JF, Xi XK, Wang WH. NMR signature of evolution of ductile-to-brittle transition in bulk metallic glasses. *Phys Rev Lett.* 2011;107:236403.
56. Jiang WH, Atzmon M. Room-temperature flow in a metallic glass—Strain-rate dependence of shear-band behavior. *J Alloys Compd.* 2011;509:7395–9.
57. Okumura H, Inoue A, Masumoto T. Glass transition and viscoelastic behaviors of La₅₅Al₂₅Ni₂₀ and La₅₅Al₂₅Cu₂₀ amorphous alloys. *Mater Trans.* 1991;32:593–8.
58. Okumura H, Chen HS, Inoue A, Masumoto T. Sub- T_g mechanical relaxation of a La₅₅Al₂₅Ni₂₀ amorphous alloy. *J Non Cryst Solids.* 1991;130:304–10.
59. Hunt AG. Fragility of liquids using percolation-based transport theories—correlation between limiting slope of the viscosity and non-exponentiality of relaxation. *J Non Cryst Solids.* 2000;274:93–101.
60. Ferrari L, Mott NF, Russo GA. Defect theory of the viscosity in glass-forming liquids. *Philos Mag A.* 1989;59:263–72.
61. Berlev A, Bobrov O, Khonik V, Csach K, Juríková A, Miškuf J, Neuhäuser H, Yazvitsky M. Viscosity of bulk and ribbon Zr-based glasses well below and in the vicinity of T_g : a comparative study. *Phys Rev B.* 2003;68:132203.
62. Csach K, Bobrov O, Khonik V, Lyakhov S, Kitagawa K. Relationship between the shear viscosity and heating rate of metallic glasses below T_g . *Phys Rev B.* 2006;73:092107.
63. Na JH, Demetriou MD, Johnson WL. Fragility of iron-based glasses. *Appl Phys Lett.* 2011;99:161902.
64. Tsyplakov AN, Mitrofanov YP, Makarov AS, Afonin GV, Khonik VA. Determination of the activation energy spectrum of structural relaxation in metallic glasses using calorimetric and shear modulus relaxation data. *J Appl Phys.* 2014;116:123507.
65. Tsyplakov AN, Mitrofanov YP, Khonik VA, Kobelev NP, Kaloyan AA. Relationship between the heat flow and relaxation of the shear modulus in bulk PdCuP metallic glass. *J Alloys Compd.* 2015;618:449–54.
66. Primak W. Kinetics of processes distributed in activation energy. *Phys Rev.* 1955;100:1677–89.
67. Gibbs MRJ, Evetts JE, Leake JA. Activation energy spectra and relaxation in amorphous materials. *J Mater Sci.* 1983;18:278–88.
68. Khonik SV, Granato AV, Joncich DM, Pompe A, Khonik VA. Evidence of distributed interstitialcy-like relaxation of the shear modulus due to structural relaxation of metallic glasses. *Phys Rev Lett.* 2008;100:065501.
69. Khonik VA, Kitagawa K, Morii H. On the determination of the crystallization activation energy of metallic glasses. *J Appl Phys.* 2000;87:8440.
70. Jiao W, Wen P, Peng HL, Bai HY, Sun BA, Wang WH. Evolution of structural and dynamic heterogeneities and activation energy distribution of deformation units in metallic glass. *Appl Phys Lett.* 2013;102:101903.